Multiplet and intrashell transitions in resonant radiative capture by F II

Ibraheem Nasser

Physics Department, King Fahd University of Petroleum and Minerals, Dhahran 31261, Saudi Arabia

R. Bellantone and Y. Hahn

Physics Department, University of Connecticut, Storrs, Connecticut 06269

A detailed analysis of the resonant radiative capture process by F II is carried out in the low-energy region. Contributions from the intrashell excitation modes with $\Delta n = 0$ and $\Delta l = 1$ are estimated. In addition, several peaks in the cross sections are found near the elastic threshold ^3P that correspond to the excitation transitions among the ground-state multiplets, with $\Delta n = 0$, $\Delta l = 0$. They are important for temperatures below 0.1 Ry. The $\Delta n = 0$, $\Delta l = 1$ contribution is large at higher temperatures, in the region of 1 Ry, where the $\Delta n \neq 0$ mode is also present. Cross sections for the direct radiative recombination are estimated to be very large for temperatures below 0.2 Ry.

I. INTRODUCTION

The dielectronic-recombination (DR) process is important in determining the ionization balance of nonequilibrium plasmas, and much work has been done in recent years both theoretically and experimentally in the evaluation of the rate coefficients for different ionic species that are present in plasmas.[1,2] Because of the complexity in the calculation of the rates, only a limited number of ions has been treated thus far, although the list is growing steadily. Most of the ions studied are of high charge states, where the Coulombic field of the core plays a dominant role. The near-neutral systems with a large number of electrons are more difficult to analyze, because of the relatively stronger electron-electron correlations. We examined Mg^+, Ca^+, and C^+ previously,[3-5] where the effect of external electric field was also important.[6]

In this paper, we report on the study of the F II ion at low energies ($e_c \leq 1.5$ Ry), below the first excitation threshold. This ion, present in the earth's upper atmosphere as one of the pollutants, presumably plays a crucial role in changing the composition of ionosphere and depleting the ozone layer. Together with the excitation and ionization rates, the electron capture by F II should be useful in understanding the elementary processes which are taking place in our upper atmosphere, where the temperature can be as high as 0.1 Ry and the resonance states up to $\sim 1.0–1.5$ Ry may therefore contribute. This is the first in a series of studies on the singly ionized species which are assumed to be important, such as C II, N II, O II, and also S II, Cl II, and P II.

The F II ion has many interesting properties to warrant detailed investigation. The spectral region above the elastic threshold is densely populated with many resonances, and the usual distinction between the intra- and intershell excitation transitions disappears. The $\Delta n \neq 0$ intershell excitation mode appears at the same energy region where the intrashell excitation contribution is dominant. The former is usually a higher-energy mode, but

not in F II. The ground-state configuration is split into three terms, and the collisional transitions among these levels also produce additional captures. Thus sizable contribution to the total cross sections and rates is expected from this very-low-energy region.

It is important to emphasize the fact that DR cross-section and rate calculations generally fall into three different categories in terms of the required accuracy of the quantities. (a) For plasma modeling the currently desired accuracy is roughly at $\pm 20\%$ level, partly because of the large quantity of data needed not only for the capture but also for the excitation and ionization rates. (b) For analysis of collision experiments, approximately $\pm 10\%$ level of reliability may be sufficient, especially when difficult coincidence measurements are involved with very low counting rates, while (c) for plasma diagnostics only a small number of resonances are usually involved and desired accuracy could be $\pm 5\%$ or better. In almost all cases, the basic constraint is placed by practical computational limitations, rather than basic theoretical deficiencies.

In Sec. II we will briefly summarize the theoretical method adopted in the evaluation of the DR cross sections and rate coefficients. The results for the ($\Delta n = 0$, $\Delta l = 1$) case are presented in Sec. III. The more exotic cases of ($\Delta n = 0$, $\Delta l = 0$) and ($\Delta n \neq 0$) excitations are summarized in Sec. IV.

II. THEORETICAL PROCEDURE

DR is a two-step higher-order resonance process, in which a target ion (i) is first collisionally excited by a projectile electron to form an intermediate resonance state (d). The intermediate state may subsequently stabilize itself by radiation emission to a final state (f), or by Auger emission of electron to states (i'). In the isolated resonance approximation, the expressions for the DR cross sections (in units of πa_0^2) and rates for given initial and intermediate states are given by[1,2]

$$\overline{\sigma}(i \rightarrow d) = \frac{1}{\Delta e_c} \frac{4\pi \, \text{Ry}}{e_c(\text{Ry})} \tau_0 V_a(i \rightarrow d)\omega(d) \quad (1)$$

where the overbar denotes an energy average over the bin size Δe_c, and

$$\alpha(kT; i \rightarrow d) = \left[\frac{4\pi \, \text{Ry}}{kT} \right]^{3/2} V_a(i \rightarrow d)\omega(d)a_0^3 e^{-e_c/kT} \quad (2)$$

where $V_a(i \rightarrow d)$ is the radiationless excitation-capture probability and, by detailed balance, related to the Auger emission probability $A_a(d \rightarrow i)$ by $V_a = (g_d/2g_i)A_a(d \rightarrow i)$, where g_d and g_i are the statistical weights of the intermediate and initial rates, respectively. $\omega(d)$ is the fluorescence yield of the state d, $\omega(d) = \Gamma_r/\Gamma(d)$ where $\Gamma(d) = \Gamma_r + \Gamma_a$ with $\Gamma_a = \sum_i A_a(d \rightarrow i)$ and $\Gamma_r = \sum_f A_r(d \rightarrow f)$. Here, A_r is the radiative transition probability, and a_0 and τ_0 are the

Bohr radius and the atomic unit of time. Finally, the total DR cross sections and rates are obtained by summing over the intermediate states, as

$$\overline{\sigma}(i) = \sum_d \overline{\sigma}(i \rightarrow d) , \quad (3)$$

$$\alpha(kT; i) = \sum_d \alpha(kT; i \rightarrow d) . \quad (4)$$

The initial excitation capture for the ground-state multiplets, (i), is described as follows:

$$(1s^2 2s^2 2p^4 = i) + k_c l_c \rightarrow (1s^2 2s 2p^5 nl = d)$$

$$(\Delta n = 0, \quad \Delta l = 1) , \quad (5a)$$

$$(1s^2 2s^2 2p^4 = i) + k_c' l_c' \rightarrow (1s^2 2s^2 2p^4 = i')nl$$

$$(\Delta n = 0, \quad \Delta l = 0) , \quad (5b)$$

$$(1s^2 2s^2 2p^4 = i) + k_c'' l_c'' \rightarrow (1s^2 2s^2 2p^3)nln'l'$$

$$(\Delta n \neq 0, \quad n, n' \geq 3) , \quad (5c)$$

which are usually followed by radiative decays

$$(1s^2 2s 2p^5 nl = d) \rightarrow (1s^2 2s^2 2p^4 nl) + \gamma(2p \rightarrow 2s)$$

$$\rightarrow (1s^2 2s 2p^5 n'l') + \gamma(nl \rightarrow n'l') , \quad (6a)$$

and

$$(1s^2 2s^2 2p^4 = i')nl \rightarrow (1s^2 2s^2 2p^4 = i')n'l'$$

$$+ \gamma(nl \rightarrow n'l') , \quad (6b)$$

with $n' \geq 2$.

The intermediate resonance states d in (5a) are given in LS coupling as $|d\rangle = |[(1s^2 2s 2p^5)^{1,3}P, nl]LS\rangle$, while the initial ground-state configuration is given by
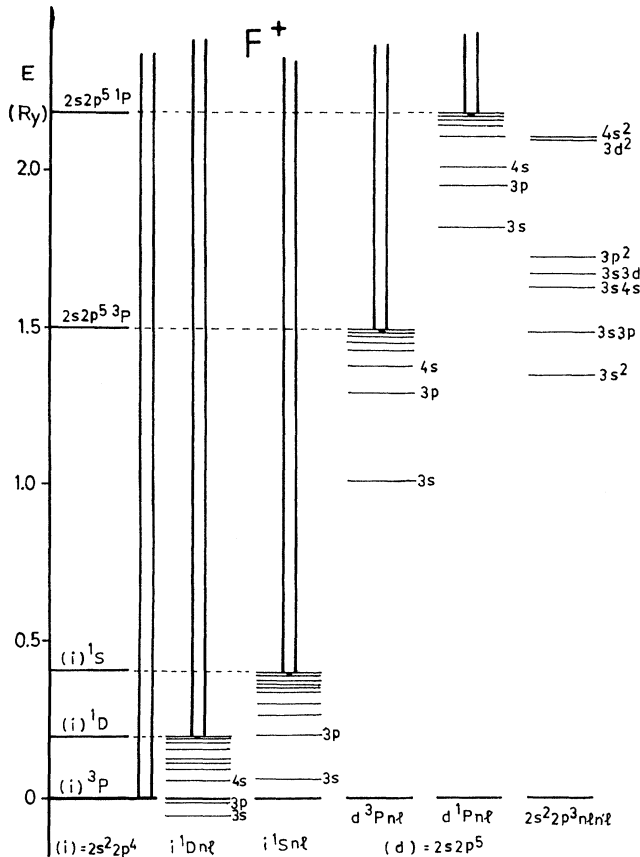
FIG. 1. Energy levels relevant to DR process for the F II ions are given, from which all possible radiative and Auger transitions for the individual intermediate resonance states may be determined. The spectrum is given in the configuration averaged positions to indicate their rough locations. The actual calculations are carried out using the correct term energies, however.

TABLE I. Allowed Auger transitions are listed for the $\Delta n = 0$, $\Delta l = 0$ and $\Delta n = 0$, $\Delta l = 1$ cases. The transitions marked with an asterisk are small because either the casade corrections are very large or LS selection rules forbid radiative and Auger transitions. n_m = the minimum allowed value for n.

d	L	n_m	i	l_c
(a) $\Delta n = 0$, $\Delta l = 0, 1$				
$[(^1P)nl]^2L$	$l, l \pm 1$	3	i_1, i_2, i_3	$l \pm 1$
$[(^3P)nl]^2L$	$l, l \pm 1$	3	i_1, i_2, i_3	$l \pm 1$
$[(^3P)nl]^4L$	$l, l \pm 1$	3	i_1	$l \pm 1$
$[(^1P)nl]^2L$	$l, l \pm 1$	3	i_4	$l, l \pm 2$
(b) $\Delta n = 0$, $\Delta l = 0$				
$[(^1S)ns]^2L$	0	3	i_1	$0^*, 2^*, 4^*$
	0	4	i_2	$0^*, 2, 4^*$
$[(^1S)np]^2L$	1	3	i_1	$1^*, 3^*$
	1	4	i_2	$1^*, 3^*$
$[(^1S)nd]^2L$	2	3	i_1	$0^*, 2^*, 4^*$
	2	3	i_2	$0, 2, 4$
$[(^1D)ns]^2L$	2	4	i_1	$0^*, 2^*, 4^*$
$[(^1D)np]^2L$	1, 2, 3	4	i_1	$1, 3$
$[(^1D)nd]^2L$	$0^*, 1, 2, 3^*, 4^*$	3	i_1	$0, 2, 4^*$

TABLE II. Values of $\bar{\sigma}^{DR}$ vs e_c (Ry) are given for the initial states i_1, i_2 with the ($\Delta n = 0$, $\Delta l = 0$) mode, and i_1, i_2, and i_3 with the ($\Delta n = 0$, $\Delta l = 1$) mode. $\bar{\sigma}^{DR}$ are given in units of cm^2, and $\Delta e_c = 0.01$ Ry.

e_c (Ry)	$\Delta n = 0$ $\Delta l = 0$		$\Delta n = 0$ $\Delta l = 1$		
	i_1	i_2	i_3	i_2	i_1
0.05	0.287×10^{-20}				
0.07	0.775×10^{-21}				
0.08		0.898×10^{-21}			
0.10		0.356×10^{-21}			
0.11	0.489×10^{-21}				
0.12	0.348×10^{-21}				
0.14	0.453×10^{-21}	0.203×10^{-21}			
0.15	0.114×10^{-21}	0.168×10^{-21}			
0.16	0.303×10^{-21}				
0.17	0.986×10^{-22}	0.215×10^{-21}			
0.18	0.924×10^{-22}	0.509×10^{-22}			
0.19		0.155×10^{-21}			
0.20		0.442×10^{-22}			
0.21		0.417×10^{-22}			
0.29	0.488×10^{-23}				
0.34	0.333×10^{-23}				
0.36	0.180×10^{-23}				
0.38	0.199×10^{-23}				
0.39	0.135×10^{-23}				
0.40	0.137×10^{-23}				
0.73			0.102×10^{-19}		
0.86			0.117×10^{-19}		
0.95			0.775×10^{-20}	0.940×10^{-20}	
0.98			0.105×10^{-19}		
1.01			0.735×10^{-20}		
1.02			0.109×10^{-20}		
1.03			0.107×10^{-19}		
1.04			0.833×10^{-20}		
1.05			0.181×10^{-19}		
1.06			0.191×10^{-19}		
1.07			0.781×10^{-19}		
1.08			0.489×10^{-17}	0.780×10^{-20}	
1.14			0.357×10^{-19}		0.108×10^{-19}
1.17				0.729×10^{-20}	
1.19				0.109×10^{-20}	
1.20				0.784×10^{-20}	
1.23				0.694×10^{-20}	
1.24				0.120×10^{-20}	
1.25				0.668×10^{-20}	
1.26				0.779×10^{-20}	
1.27				0.109×10^{-19}	0.353×10^{-19}
1.28				0.154×10^{-19}	
1.29				0.530×10^{-19}	
1.30				0.617×10^{-18}	
1.36				0.599×10^{-20}	0.914×10^{-20}
1.39					0.954×10^{-19}
1.41			0.334×10^{-20}		
1.42					0.872×10^{-20}
1.43					0.821×10^{-19}
1.44					0.728×10^{-19}
1.45					0.137×10^{-18}
1.46					0.395×10^{-19}
1.47					0.283×10^{-18}
1.48					0.472×10^{-18}
1.49					0.326×10^{-17}
1.54			0.252×10^{-19}		
1.63			0.394×10^{-20}	0.867×10^{-20}	

TABLE II. (Continued).

e_c (Ry)	$\Delta n=0$ $\Delta l=0$		$\Delta n=0$ $\Delta l=1$		
	i_1	i_2	i_3	i_2	i_1
1.65			0.163×10^{-18}		
1.66			0.291×10^{-19}		
1.69			0.398×10^{-20}		
1.70			0.308×10^{-18}		
1.71			0.197×10^{-19}		
1.72			0.293×10^{-18}		
1.73			0.269×10^{-19}		
1.74			0.434×10^{-18}		
1.75			0.461×10^{-18}		
1.76			0.106×10^{-17}	0.313×10^{-19}	
1.82					0.819×10^{-20}
1.85				0.795×10^{-20}	
1.87				0.990×10^{-19}	
1.88				0.303×10^{-19}	
1.91				0.776×10^{-20}	
1.92				0.184×10^{-18}	
1.93				0.295×10^{-19}	
1.94				0.187×10^{-18}	
1.95				0.436×10^{-19}	0.145×10^{-19}
1.96				0.344×10^{-18}	
1.97				0.557×10^{-18}	
1.98				0.238×10^{-17}	
2.04					0.725×10^{-20}
2.06					0.329×10^{-21}
2.07					0.119×10^{-19}
2.10					0.686×10^{-20}
2.11					0.389×10^{-21}
2.12					0.129×10^{-19}
2.13					0.714×10^{-20}
2.14					0.262×10^{-19}
2.15					0.202×10^{-19}
2.16					0.710×10^{-19}
2.17					0.346×10^{-18}

$|i\rangle=|[(1s^22s^22p^4)^3P, {}^1D, {}^1S, \ k_cl_c]L'S'\rangle$. We have $L=L'$ and $S=S'$ for the Auger transition mediated by electron-electron interactions. The various channels reached by Auger transition are defined by $i_l\equiv(i)^3P$, $i_2\equiv(i)^1D$, $i_3\equiv(i)^1S$, and $i_4\equiv(d)^3P$.

The following procedure was adopted in the present work for the calculation of DR cross sections and the rate coefficients.

(i) All the ionic bound-state orbitals were generated using nonrelativistic Hartree-Fock (NRHF) code, in single-configuration approximation.

(ii) The continuum orbitals used in the evaluation of Auger transitions A_a are calculated using NRHF in the single-channel distorted wave method.

(iii) LS coupling was employed throughout the calculations, where inner-shell orbitals are coupled first. (Some of the earlier calculations employed the active-electron coupling scheme.[1,2])

(iv) For a given intermediate state there may be more than one Auger channel allowed by energy, parity, and angular momentum conservation. Using energies obtained from Cowan's RCG code and from the available spectroscopic data, the threshold values of $n=n_m$ were determined for each series of Auger channels. Wherever possible, data tables[7] were consulted to adjust energies. This is especially critical when the transition energies are small.

(v) Cascade corrections are very important when the Auger probabilities following a given radiative transition are very large.

Figure 1 shows the energy levels relevant to DR process for F II ions, from which possible radiative and Auger transitions for the individual intermediate resonance states may be determined. The spectrum is given in the configuration averaged positions to indicate their rough locations. However, the actual calculations used the term energies. The cross sections and rate coefficients we present here should be reliable at the level of $\pm10\%$;

this estimate is arrived at by noting that, because of the dominance of A_a over A_r, the DR cross sections are basically proportional to A_r, which are much more accurately determined than A_a. This feature is generally valid for all cases involving intrashell excitations. The data presented here should therefore be useful for modeling and analysis of accurate collision experiments.

III. THE INTRASHELL CONTRIBUTION

The allowed autoionization transitions for the doubly excited states $[(1s^2 2s 2p^5)^{1,3}P, nl]^{2,4}L \rightarrow [(1s^2 2s^2 2p^4)^3P, {}^1D, {}^1S, k_c l_c]$ are summarized in Table I, corresponding to the $\Delta n = 0$, $\Delta l = 1$ mode in LS coupling. The initial-state configuration $1s^2 2s^2 2p^4$ is split by $\Delta E = 0.19$ Ry for ^1D and $\Delta E = 0.41$ Ry for ^1S as measured from the ground ^3P state. The excitation threshold energies for the intermediate states are $E_{th} = 1.50$ Ry for ^3P and $E_{th} = 2.18$ Ry for ^1P. The continuum electron orbital angular momenta are determined by the parity and other conservation laws. The lowest n allowed by energy conservation is $n_m = 3$ for all the channels described in Table I.

The doubly excited intermediate states may also decay radiatively to states $1s^2 2s^2 2p^4 nl$, $1s^2 2s^2 2p^5$, and $1s^2 2s^2 2p^4 n'l'$. The first of these is the dominant one, and the second state is less important due to the well-known behavior of A_r with respect to n, $A_r \sim n^{-3}$. The cascade correction makes the contribution from the third state negligible.

Calculations were carried out explicitly for $n \leq 12$, and the contribution from $n \geq 12$ was estimated by extrapolation. (The extrapolation was carried out for each A_a and A_r, and then they were combined to obtain $\bar{\sigma}$ and α.) We note that the radiative and the Auger transitions do not scale well as n^{-3} for $n < 10$. The fact that the fluorescence yields $\omega(n)$ were small means that the contribution from high Rydberg states (HRS) was important. Contributions from $n \leq 1000$ were summed, for $l \leq 5$.

The cross sections are given in Table II as functions of the continuum electron energy e_c(Ry) for the three different initial states, and Fig. 2 summarizes the rates. The rates for the direct radiative recombination (RR) were also estimated using the result of Ref. 8. The RR process competes with DR and dominates at $kT \leq 0.5$ Ry. The radiative recombination rate at $kT = 1$ Ry is estimated to be $\sim 1.5 \times 10^{-12}$ cm^2/sec, which is roughly $\frac{1}{2}$ of the DR rates calculated here. The interference between the RR and DR amplitudes is not included, as its effect is expected to be small for the extremely narrow resonances we have.

IV. MULTIPLET TRANSITIONS AND INTERSHELL CONTRIBUTIONS

A. $\Delta n = 0$, $\Delta l = 0$ (multiplet transitions)

The selection rules in LS coupling for autoionization transitions in the doubly excited states $[(1s^2 2s^2 2p^4)^1S, {}^1D, nl]^2L \rightarrow [(1s^2 2s^2 2p^4)^3P, {}^1D, k_c l_c]$ are also summarized in Table I. All the states with $l > 2$ are allowed to decay by radiative transitions but the cascade corrections
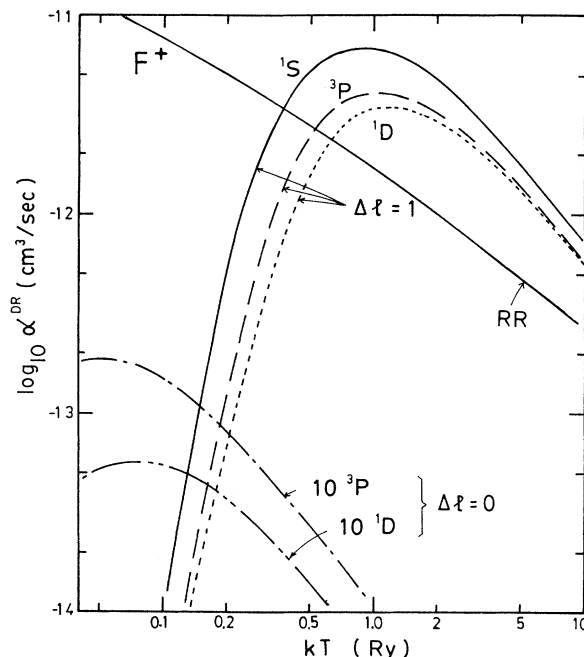
FIG. 2. α^{DR} vs kT are presented for the $\Delta n = 0$, $\Delta l = 1$ mode of excitation. The radiative recombination (RR) rate is also given for comparison. The low-temperature end shows the DR contribution from the multiplet mode.

reduce $\bar{\sigma}$ to negligible values. Thus the transitions marked with asterisks in Table I are either reduced by the cascade effect or not allowed by radiative or Auger transitions.

The multiplet resonance captures provide sizable rates at very low temperature, peaking at $kT \leq 0.1$ Ry, and comparable in magnitude with the ($\Delta n = 0$, $\Delta l = 1$) contribution at 0.1 Ry, although the latter mode is nearly 100 times larger at its peak near $kT \sim 1.0$ Ry (Fig. 2). At $kT \sim 0.05$ Ry, the $\Delta l = 0$ mode is nearly 100 times larger than that for $\Delta l = 1$. The direct radiative recombination rate[8] dominates at this temperature, however; we obtain the RR rate of approximately 6×10^{-12} cm^3/sec at $kT = 0.15$ Ry. Thus the effect of multiplet transitions can show up prominently only in a precision DR cross-section experiment in which the characteristic light emission is detected in coincidence with the charge state of the residual captured ion.

B. $\Delta n \neq 0$ (intershell transitions)

This excitation mode usually contributes at much higher temperature because of large excitation energies required. However, for F II, the lowest allowed intermediate state $1s^2 2s^2 2p^3 3s^2$ lies below the $1s^2 2s 2p^5 nl (n \rightarrow \infty)$ threshold of the intrashell excitation mode. In fact, many other states in LS coupling lie in the energy region $e_c \sim 1.0$ Ry. The distinction between the intrashell and intershell excitation modes disappeared. This is rather unexpected for such light ions as F, since this feature is generally believed to set in for ions with 12
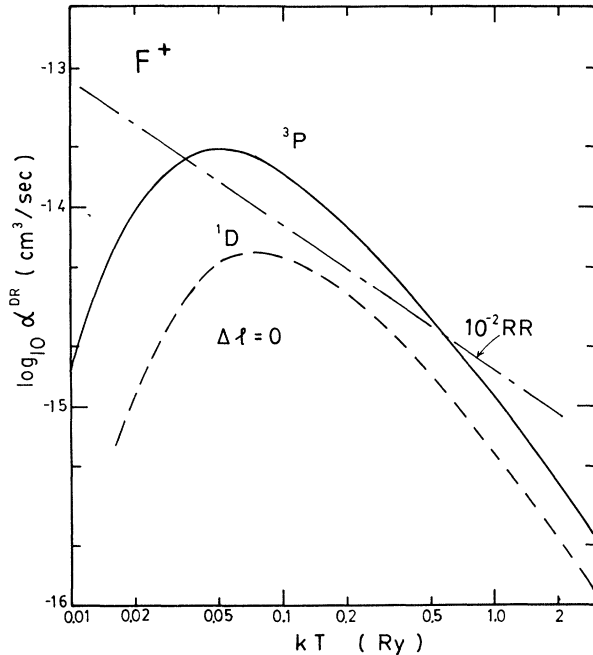
FIG. 3. α^{DR} vs kT are given for the $\Delta n = 0$, $\Delta l = 0$ mode of excitation. The radiative recombination rates are given, after scaling it down by 10^{-2}.

TABLE III. Contribution to the total DR of the $\Delta n \neq 0$ mode by the state $(1s^2 2s^2 2p^3 3s^2)^4 S^2 D^2 P$ is presented. α is given in units of cm^3/sec, at $kT = 1$ Ry. $\Delta e_c = 0.01$ Ry. $l_c = 1$.

i	d	e_c Ry	$\bar{\sigma}$ (cm^2)	$\alpha(kT = 1.0$ Ry)
i_1	^4S	1.14	0.686×10^{-21}	0.616×10^{-15}
	^2D	1.45	0.155×10^{-20}	0.130×10^{-14}
	^2P	1.68	0.857×10^{-21}	0.661×10^{-15}
			0.309×10^{-20} (total)	0.258×10^{-14} (total)
i_2	^2D	1.26	0.286×10^{-20}	0.252×10^{-14}
	^2P	1.48	0.307×10^{-21}	0.255×10^{-15}
			0.316×10^{-20} (total)	0.277×10^{-14} (total)
i_3	^2P	1.26	0.150×10^{-20}	0.132×10^{-14}
			0.150×10^{-20} (total)	0.132×10^{-14} (total)

or more electrons. We made an estimate of the contribution to $\bar{\sigma}$ and α of this and several other states. They are reduced in magnitude by the cascade corrections, in which initial radiative decays lead to states which are Auger unstable. The only radiative transitions that contribute significantly to DR are to the final states $(1s^2 2s^2 2p^4)^1 D 3s$ and $3p$. Sample results for the state $1s^2 2s^2 2p^3 3s^2$ are given in Table III.

For comparison, the cross sections for the intermediate states $(1s^2 2s 2p^4)3l$, in the case of $(\Delta n = 0, \Delta l = 1)$ mode and for the initial states i_1, i_2, and i_3 are 0.133×10^{-18} 0.157×10^{-18}, and 0.214×10^{-18}, respectively. The values in Table III are about 2% of the above. More extensive calculations are needed to estimate the $\Delta n \neq 0$ contribution, but previous studies[2] on other similar ions indicate that the total contribution from this mode may be 10–20 % of that from the $\Delta n = 0$ mode. (This may be a lower estimate because of the breakdown in the distinction of two excitation modes discussed above.)

V. DISCUSSIONS

Three distinct excitation modes are studied: ($\Delta n = 0$, $\Delta l = 0$), ($\Delta n = 0$, $\Delta l = 1$), and ($\Delta n \neq 0$). In the case of ($\Delta n = 0$, $\Delta l = 0$), the most significant contribution at low energy ($e_c \leq 0.2$ Ry) comes from the transitions $(i_2)nl \rightarrow (i_1), k_c l_c$, where $n \leq 20$ and small l ($l \leq 2$). The ($\Delta n = 0$, $\Delta l = 1$) mode contributes the most in the temperature region $kT \leq 1.0$ Ry. Unlike in the case of highly charged ions, additional complications are introduced by the presence of resonances in this energy region which correspond to the $\Delta n \neq 0$ mode. Presumably, such a situation is more common to ions with more than 11 electrons.

trons. Further work[9] is in progress to examine the "mirror" ion N II, with two $2p$ electrons rather than two $2p$ holes, which is another important ion present in the upper atmosphere.

The effect of possible electric field on the rate coefficients can be large for the mode ($\Delta n = 0$, $\Delta l = 1$), but is not expected to be significant for the other two modes considered here, where the contributions from high Rydberg states are small. The contribution of the direct radiative recombination to the total capture rates dominates at low temperatures. The interference effect between the RR and DR amplitudes is expected to be small, mainly because of the small resonance widths involved; it is important only when the RR amplitude varies rapidly with energy within the range of the resonance width, that is, in the region where the RR amplitude decreases rapidly. Perhaps more important may be the effect of resonance overlap for states with very large n (and for cases in which small external field perturbations are present) and the interference between the contributions from different excitation modes. We have not included these effects in the present calculation.

Similar comments could be made on the effect of configuration interaction. Due to the unitary nature of the mixing matrix, the total cross sections are generally much less sensitive to the mixing, although the individual states are sometimes very much affected by it. The dependence of our result on the coupling scheme used is also very weak in so far as the total cross section is concerned. The difference between the LS and LSJ coupling is expected to be small for our system, F I, because of the weak spin-orbit coupling. Therefore we neglected these and other possible complications in the present calculation. (The intermediate state $2s2p^6 \, ^2S$ lies 1.54 Ry above i_1, but its contribution from i_1 is identically zero.)

ACKNOWLEDGMENTS

[1]Y. Hahn, Adv. At. Mol. Phys. **21**, 123 (1985).

[2]Y. Hahn and K. LaGattuta, Phys. Rep. **166**, 195 (1988).

[3]K. LaGattuta and Y. Hahn, Phys. Rev. Lett. **50**, 668 (1983).

[4]I. Nasser and Y. Hahn, Phys. Rev. A **30**, 1558 (1984).

[5]K. LaGattuta and Y. Hahn, At. Mol. Phys. **15**, 2101 (1982).

[6]K. LaGattuta and Y. Hahn, Phys. Rev. Lett. **51**, 558 (1983).

[7]S. Bashkin and J. O. Stoner, Jr., in *Atomic Energy Levels and Grotrian Diagrams* (North-Holland, Amsterdam, 1977).

[8]D. McLaughlin and Y. Hahn, Phys. Rev. A **43**, 1313 (1991).

[9]I. Nasser and Y. Hahn (unpublished).